Current-induced torques in textured Rashba ferromagnets

E. van der Bijl* and R. A. Duine
Institute for Theoretical Physics, Utrecht University, Leuvenlaan 4, 3584 CE Utrecht, The Netherlands
(Received 25 May 2010; published 5 September 2012)

In systems with small spin-orbit coupling, current-induced torques on the magnetization require inhomogeneous magnetization textures. For large spin-orbit coupling, such torques exist even without gradients in the magnetization direction. Here, we consider current-induced torques in ferromagnetic metals with both Rashba spin-orbit coupling and inhomogeneous magnetization. We first phenomenologically construct all torques that are allowed by the symmetries of the system, to first order in magnetization-direction gradients and electric field. Second, we use a Boltzmann approach to calculate the spin torques that arise to second order in the spin-orbit coupling. We apply our results to current-driven domain walls and find that the domain-wall mobility is strongly affected by torques that result from the interplay between spin-orbit coupling and inhomogeneity of the magnetization texture.

DOI: 10.1103/PhysRevB.86.094406 PACS number(s): 75.60.Ch

I. INTRODUCTION

Current-induced torques on the magnetization in conducting ferromagnets are one of the main topics of research in spintronics. In addition to being fundamentally interesting, these torques are also key to developments in memory technology.[1] Current-induced torques can be used to move domain walls through a ferromagnetic wire. When a domain wall is present the direction of the magnetization depends on the position in the wire. This spatial dependence of the magnetization gives rise to a mismatch between the electron spin polarization and local magnetization, resulting in adiabatic reactive[2,3] and dissipative (also known as nonadiabatic) spin transfer torques (STTs).[4–9] The occurrence of these two spin torques is well estabished but their relative magnitude, parametrized by the dimensionless parameter β which describes the relative strength of the dissipative torque with respect to the reactive one, is hard to measure[10] and calculate.[11]

That there exist other current-induced torques related to spin-orbit (SO) coupling of the carriers has been proposed recently.[12–15] In these works systems with SO coupling and homogeneous magnetization are considered. Recent experiments can be interpreted using these current-induced torques originating from the SO coupling of the carriers[16–20] that, unlike the adiabatic STT mentioned above, do not require magnetization gradients. (Note, however, that these observations can also be described via the spin-Hall effect in Pt as argued in Ref. 17.) For Rashba SO coupling, two current-induced torques have been found in the situation where there is no magnetization gradient. In the experimental works, however, a domain wall is present. This implies that the description in terms of a homogeneous magnetization is incomplete, and a more systematic description including both SO coupling and an inhomogeneous magnetization is called for.

It is the purpose of this work to give such an inclusive description that incorporates both SO coupling and inhomogenous magnetization textures. For definiteness, we focus on the Rashba SO coupling. In Sec. II we consider all current-induced torques which are allowed by the symmetries of the system. As the number of allowed torques is considerable, and because the symmetry considerations do not yield their relative magnitudes, we investigate these within a semiclassical Boltzmann description (Sec. III). In Sec. IV and V we respectively present results for the conductivity and current-induced torques that result from this approach. In Sec. VI the results for the torques are used to calculate their effect on domain-wall dynamics. We find that the current-induced domain-wall velocity depends strongly on wall geometry. Furthermore, the domain-wall mobility depends strongly on the inclusion of torques that result from the interplay of SO coupling and gradients in the magnetization.

II. SYMMETRY CONSIDERATIONS

In this section we use symmetry considerations to obtain all allowed current-induced torques. To illustrate our method we begin with the adiabatic spin torques in the absence of SO coupling. Subsequently we investigate the situation with SO coupling. We use the s-d model since this is a convenient model to get a qualitative description of current-induced torques. In this model the magnetization resides on the d orbitals and transport is due to the mobile s electrons. We investigate the system well below the Curie temperature, which means the magnetization is represented using a unit-vector field since fluctuations in its magnitude are negligible.

A. Absence of spin-orbit coupling

Within the s-d model the Hamiltonian is given by

$$\mathcal{H}_{sd} = \mathcal{H}_0(\boldsymbol{x},\boldsymbol{p}) - \frac{\Delta}{2}\boldsymbol{m}\cdot\boldsymbol{s}, \tag{1}$$

where $\mathcal{H}_0$ is the Hamiltonian that describes the motion of the itinerant electrons and depends on electron momentum $\boldsymbol{p}$ and position $\boldsymbol{x}$. We have an exchange coupling between the magnetic texture $\boldsymbol{m}(\boldsymbol{x},t)$ and the electron spin $\boldsymbol{s}(t)$ specified by the exchange splitting Δ. The total Hamiltonian $\mathcal{H}_{sd}$ is invariant under two *independent* rotations of the spin and physical space, parametrized by the rotation matrices $\mathcal{R}_{\mathrm{S}}^{ij}$ and $\mathcal{R}^{ij}$, respectively. (We neglect the coupling between the magnetization and the orbit of the electrons that occurs via the Lorentz force. We neglect this effect for the moment because the magnetic field induced by the magnetization is very small.) Moreover, in this description we neglect the ionic lattice. We

explicitly have for the rotations

$$\tilde{s}^i = \mathcal{R}_{\rm S}^{ij} s^j, \quad \tilde{m}^i = \mathcal{R}_{\rm S}^{ij} m^j; \tag{2}$$

$$\tilde{x}^i = \mathcal{R}^{ij} x^j, \quad \tilde{p}^i = \mathcal{R}^{ij} p^j. \tag{3}$$

Note that we use the summation convention of summing over repeated indices. The invariance of the Hamiltonian implies that $\mathcal{H}_{sd}(\tilde{\boldsymbol{p}},\tilde{\boldsymbol{x}},\tilde{\boldsymbol{s}},\tilde{\boldsymbol{m}}) = \mathcal{H}_{sd}(\boldsymbol{p},\boldsymbol{x},\boldsymbol{s},\boldsymbol{m})$. This means that these symmetries should be respected at the level of the equations of motion. We are interested in the (linear-response-) current-induced torques; hence our expressions for the torques should be linearly dependent on the applied electric field $\boldsymbol{E}$. The possible torques that are first order in the electric field $\boldsymbol{E}$, which transforms under the action of $\boldsymbol{R}$, should involve an inner product with another vector that transforms under the same rotation and in this way creates an invariant scalar. The only other vector that transforms in this way for this system is the gradient $\boldsymbol{\nabla}$ that acts on the magnetization. These constraints lead to the two possible current-induced torques

$$\left.\frac{\partial \boldsymbol{m}}{\partial t}\right|_{\rm ST} \propto (\boldsymbol{E}\cdot\boldsymbol{\nabla})\boldsymbol{m} + \beta \boldsymbol{m}\times(\boldsymbol{E}\cdot\boldsymbol{\nabla})\boldsymbol{m}. \tag{4}$$

For a treatment of spin transfer torques that incorporates the symmetries of the lattice see Ref. 21. These terms are frequently written in terms of the current but we choose to put in the electric field here as the external perturbation, to be consistent with the rest of this paper. Note the parameter β, which is defined as the ratio of the dissipative and reactive spin transfer torques.

The two torques in Eq. (4) are mutually perpendicular. Moreover, they transform differently under time reversal, since they differ by a factor $\boldsymbol{m}$ which is odd under time reversal. This difference in behavior under time-reversal symmetry implies that the torques form a pair where one is reactive and the other is dissipative.

B. Spin-orbit coupling

In the presence of SO coupling the Hamiltonian for the spin of the s electron couples the spin and the momentum of the electron. We represent SO coupling for spin-$\frac{1}{2}$ carriers via the Hamiltonian

$$\mathcal{H}_{\rm SO} = -\boldsymbol{\Omega}(\boldsymbol{x},\boldsymbol{p})\cdot\boldsymbol{s}, \tag{5}$$

where $\boldsymbol{\Omega}$ contains both the exchange interaction of Eq. (1) and SO coupling, and can be seen as a position- and momentum-dependent effective exchange splitting.

For definiteness, and motivated by experiments,[16,17] we study the simplest form of SO coupling described by the Rashba Hamiltonian[22] $\mathcal{H}_{\rm R} = -\lambda(\boldsymbol{p}\times\boldsymbol{e}_z)\cdot\boldsymbol{s}$. The Rashba coupling together with the exchange interaction results in

$$\boldsymbol{\Omega}(\boldsymbol{x},\boldsymbol{p}) = \frac{\Delta}{2}\boldsymbol{m}(\boldsymbol{x}) + \lambda\,\boldsymbol{p}\times\boldsymbol{e}_z. \tag{6}$$

Rashba SO coupling occurs in two-dimensional electron systems with inversion asymmetry along the direction perpendicular to the two-dimensional electron gas (which we choose as our z axis). The SO coupling breaks the invariance of the Hamiltonian under separate rotations of the spin and orbital parts of the motion. Total angular momentum is still conserved due to the invariance of the Hamiltonian under combined rotations of spin and physical space, parametrized by $\mathcal{R}_{\rm S}^{ij} = \mathcal{R}^{ij}$.

The linear-response matrix $L_{\rm CIT}(\boldsymbol{m},\boldsymbol{e}_z,\boldsymbol{\nabla}\boldsymbol{m})$ that describes the current-induced torques is defined by

$$\dot{m}^i = L_{\rm CIT}^{ij}(\boldsymbol{m},\boldsymbol{e}_z,\boldsymbol{\nabla}\boldsymbol{m})E^j, \tag{7}$$

where $\boldsymbol{E}$ is the electric field in the plane and $\boldsymbol{e}_z$ is a unit vector in the z direction. The linear-response matrix depends on this direction since inversion symmetry is broken along this direction. The Hamiltonian is invariant under parity transformations, which implies that the linear-response matrix should obey $-L_{\rm CIT}(\boldsymbol{m},-\boldsymbol{e}_z,-\boldsymbol{\nabla}\boldsymbol{m}) = L_{\rm CIT}(\boldsymbol{m},\boldsymbol{e}_z,\boldsymbol{\nabla}\boldsymbol{m})$. This shows that there can be torques on the magnetization without a gradient in the magnetization. These torques $\tau_{\rm ST} i = L_{ij}(\boldsymbol{m},\boldsymbol{e}_z)E^j$ have been found before[12] and are given by

$$\boldsymbol{\tau}_{\rm ST}^{(1)} \propto \boldsymbol{m}\times(\boldsymbol{E}\times\boldsymbol{e}_z); \tag{8}$$

$$\boldsymbol{\tau}_{\rm ST}^{(1\perp)} \propto \boldsymbol{m}\times[\boldsymbol{m}\times(\boldsymbol{E}\times\boldsymbol{e}_z)]. \tag{9}$$

The spin torques are perpendicular to $\boldsymbol{m}$ because it is a unit-vector field. Since the magnetization is embedded in three-dimensional space there is a two-dimensional plane perpendicular to it. This means that any spin torque $\boldsymbol{\tau}_{\rm ST}^{(i)}$ allowed by the symmetry of the system immediately defines another torque via $\boldsymbol{\tau}_{\rm ST}^{(i\perp)} = \boldsymbol{m}\times\boldsymbol{\tau}_{\rm ST}^{(i)}$. These pairs differ by a factor $\boldsymbol{m}$ which changes its sign under time reversal; hence the two torques form a reactive-dissipative pair, like the STTs in Eq. (4). In the following we will show only one of the pair. All terms to first order in the gradient of the magnetization that do not involve $\boldsymbol{e}_z$ are given by

$$\boldsymbol{\tau}_{\rm ST}^{(2)} \propto (\boldsymbol{E}\cdot\boldsymbol{\nabla})\boldsymbol{m}; \tag{10}$$

$$\boldsymbol{\tau}_{\rm ST}^{(3)} \propto [(\boldsymbol{m}\times\boldsymbol{E})\cdot\boldsymbol{\nabla}]\boldsymbol{m}; \tag{11}$$

$$\boldsymbol{\tau}_{\rm ST}^{(4)} \propto (\boldsymbol{m}\cdot\boldsymbol{E})(\boldsymbol{m}\cdot\boldsymbol{\nabla})\boldsymbol{m}; \tag{12}$$

$$\boldsymbol{\tau}_{\rm ST}^{(5)} \propto E^a(\boldsymbol{m}\times\boldsymbol{\nabla})\boldsymbol{m}^a; \tag{13}$$

$$\boldsymbol{\tau}_{\rm ST}^{(6)} \propto (\boldsymbol{m}\times\boldsymbol{E})^a(\boldsymbol{m}\times\boldsymbol{\nabla})\boldsymbol{m}^a; \tag{14}$$

$$\boldsymbol{\tau}_{\rm ST}^{(7)} \propto \boldsymbol{m}\times\boldsymbol{E}(\boldsymbol{\nabla}\cdot\boldsymbol{m}); \tag{15}$$

$$\boldsymbol{\tau}_{\rm ST}^{(8)} \propto (\boldsymbol{m}\times\boldsymbol{E})\,[\boldsymbol{m}\cdot(\boldsymbol{\nabla}\times\boldsymbol{m})]\,. \tag{16}$$

In the first line the familiar STT (Refs. 2 and 3) describing the current-induced torque in systems with inhomogeneous magnetization is obtained. Together with the dissipative STT (Refs. 4–9) that is associated with it ($\tau_{\rm ST}^{2\perp}$), those torques describe the weak-SO-coupling situation. In the second line we find a STT due to a Hall current. The other torques do not have a straightforward physical interpretation.

Up to this point we have explicitly given the torques to first order in either $\boldsymbol{e}_z$ or $\boldsymbol{\nabla}$. There are more torques that involve an even number of $\boldsymbol{e}_z$'s and are first order in $\boldsymbol{\nabla}$. We will not list them because the list will be too long to be illuminating. We proceed by actually calculating the torques in the next section. The reason we do this is twofold. First, having demonstrated the existence of many spin torques due

to the combined effects of SO coupling and magnetization gradients, we now explicitly calculate which torques occur within a semiclassical approach to the Rashba model. The second reason is to give an estimate of the relative magnitudes of the various current-induced torques which cannot be found using symmetry arguments.

III. SEMICLASSICAL FRAMEWORK

In order to investigate microscopically which current-induced torques appear for the textured Rashba ferromagnet, we use a semiclassical approach. This approach has proved its merit in the description of the anomalous Hall effect.[23] We describe the system by the Hamiltonian

$$\mathcal{H} = \frac{\boldsymbol{p}^2}{2m_e} - \boldsymbol{\Omega}(\boldsymbol{x},\boldsymbol{p})\cdot\boldsymbol{s} + E_{\mathrm{MM}}[\boldsymbol{m}], \tag{17}$$

where $\boldsymbol{\Omega}(\boldsymbol{x},\boldsymbol{p})$ is the effective Zeeman field, given in Eq. (6), which incorporates the Rashba SO coupling and the exchange coupling, and $E_{\mathrm{MM}}[\boldsymbol{m}]$ is the micromagnetic energy functional for the magnetization. Furthermore, m_e is the effective mass of the electron. The equation of motion for the spin degree of freedom is written as

$$\frac{d\boldsymbol{s}}{dt} = \frac{1}{\hbar}\boldsymbol{s}\times\boldsymbol{\Omega} - \frac{\alpha}{\hbar}\boldsymbol{s}\times(\boldsymbol{s}\times\boldsymbol{\Omega}),$$

where we introduced a damping term proportional to α that describes relaxation of the spin into the direction of the effective Zeeman field. The spin dynamics is much faster than the motion of the electrons, such that we can solve the above equation of motion up to first order in time derivatives of $\boldsymbol{\Omega}$. We obtain the following solutions:

$$\boldsymbol{s}_s = s\hat{\boldsymbol{\Omega}} + s\frac{\hbar}{\sqrt{\boldsymbol{\Omega}\cdot\boldsymbol{\Omega}}}\frac{d\hat{\boldsymbol{\Omega}}}{dt}\times\hat{\boldsymbol{\Omega}} - \frac{\hbar\alpha}{\sqrt{\boldsymbol{\Omega}\cdot\boldsymbol{\Omega}}}\frac{d\hat{\boldsymbol{\Omega}}}{dt}, \tag{18}$$

where $s=\pm1$ describe the majority ($s=+$) [minority ($s=-$)] electrons, and $\hat{\boldsymbol{\Omega}} = \boldsymbol{\Omega}/|\boldsymbol{\Omega}|$. The first term describes the adiabatic following of the effective magnetization texture by the electron spins. The other terms describe the slight mismatch of the spins with the effective magnetization. We find the dynamics of the itinerant electrons by inserting the first-order solutions of the spin degree of freedom, given in Eq. (18), into the Hamilton equations of motion for the electrons. We obtain

$$\dot{x}_s^i = \frac{\partial\epsilon_s}{\partial p^i} - s\hbar\left(\frac{\partial\hat{\boldsymbol{\Omega}}}{\partial p^i}\times\frac{d\hat{\boldsymbol{\Omega}}}{dt}\right)\cdot\hat{\boldsymbol{\Omega}} + \alpha\hbar\frac{\partial\hat{\boldsymbol{\Omega}}}{\partial p^i}\cdot\frac{d\hat{\boldsymbol{\Omega}}}{dt};$$

$$\dot{p}_s^i = -\frac{\partial\epsilon_s}{\partial x^i} + s\hbar\left(\frac{\partial\hat{\boldsymbol{\Omega}}}{\partial x^i}\times\frac{d\hat{\boldsymbol{\Omega}}}{dt}\right)\cdot\hat{\boldsymbol{\Omega}} - \alpha\hbar\frac{\partial\hat{\boldsymbol{\Omega}}}{\partial x^i}\cdot\frac{d\hat{\boldsymbol{\Omega}}}{dt} - |e|\boldsymbol{E}^i,$$

where $\epsilon_s = \boldsymbol{p}^2/2m_e - s|\boldsymbol{\Omega}|$ is the dispersion for the majority ($s=+$) [minority ($s=-$)] electrons. Note that we added an electric field to induce a transport current. The total time derivatives on $\hat{\boldsymbol{\Omega}}$ should be understood as

$$\frac{d\hat{\boldsymbol{\Omega}}}{dt} = \dot{x}_s^i\frac{\partial\hat{\boldsymbol{\Omega}}}{\partial x^i} + \dot{p}_s^i\frac{\partial\hat{\boldsymbol{\Omega}}}{\partial p^i}.$$

Now that we have this semiclassical description of the single-particle dynamics we calculate the spin torques using the Boltzmann equation for the distribution function $f_s(\boldsymbol{x},\boldsymbol{p},t)$ of the particles, which, in the relaxation-time (τ_r) approximation, is given by

$$\frac{d}{dt}f_s(\boldsymbol{x},\boldsymbol{p},t) = -\frac{f_s(\boldsymbol{x},\boldsymbol{p},t) - f^{\mathrm{FD}}(\epsilon_s)}{\tau_r}, \tag{19}$$

where $f^{\mathrm{FD}}(\epsilon) = (1+e^{\beta(\epsilon-\epsilon_F)})^{-1}$ is the Fermi-Dirac distribution function, and ϵ_F is the Fermi energy. The relaxation-time approximation is the simplest description of the Boltzmann collision integral. We make the relaxation-time approximation here for convenience. A detailed study of the collision integral in the presence of strong SO coupling is beyond the scope of this work. We refer to the work by Pesin and MacDonald in Ref. 19 for more details on the situation of homogeneous magnetization. The left-hand side in Eq. (19) should be read as

$$\frac{df_s}{dt} = \frac{\partial f_s(\boldsymbol{x},\boldsymbol{p},t)}{\partial t} + \frac{\partial f_s(\boldsymbol{x},\boldsymbol{p},t)}{\partial\boldsymbol{p}}\cdot\dot{\boldsymbol{p}}_s + \frac{\partial f_s(\boldsymbol{x},\boldsymbol{p},t)}{\partial\boldsymbol{x}}\cdot\dot{\boldsymbol{x}}_s.$$

The equation of motion for the magnetization is the Landau-Lifshitz-Gilbert (LLG) equation

$$\frac{\partial\boldsymbol{m}}{\partial t} = -\gamma\boldsymbol{m}\times\boldsymbol{H}_{\mathrm{eff}} + \alpha_G\boldsymbol{m}\times\frac{\partial\boldsymbol{m}}{\partial t} + \boldsymbol{\tau}_{sd}, \tag{20}$$

where γ is the gyromagnetic ratio and the torques due to the s-d coupling $\boldsymbol{\tau}_{sd} = \Delta/(2\hbar)\boldsymbol{m}\times\langle\boldsymbol{s}\rangle$ contain the spin torques of interest and a renormalization of the parameters in the LLG equation[4] which we discuss in this section. The current-induced torques are proportional to the electric field and will be given in Sec. V. The renormalized LLG equation we obtain is given by

$$(1-\eta)\frac{\partial\boldsymbol{m}}{\partial t} = -\gamma\boldsymbol{m}\times\boldsymbol{H}'_{\mathrm{eff}} + \alpha'_G\boldsymbol{m}\times\frac{\partial\boldsymbol{m}}{\partial t} + \boldsymbol{\tau}_{\mathrm{ST}}, \tag{21}$$

where $\boldsymbol{\tau}_{\mathrm{ST}}$ contains all terms of $\boldsymbol{\tau}_{sd}$ proportional to the electric field, $\boldsymbol{H}'_{\mathrm{eff}}$ is defined as the effective magnetic field acting on the magnetization, which acquires an additional term from the coupling to the electrons,

$$\boldsymbol{H}'_{\mathrm{eff}} = -\frac{\delta E_{\mathrm{MM}}}{\delta\boldsymbol{m}} + \alpha\frac{m_e^2a^2\lambda_R^2}{2\gamma\pi\hbar^2}\left(1+\frac{4\epsilon_F^2}{\Delta^2}\right)(\dot{\boldsymbol{m}}\cdot\boldsymbol{e}_z)\boldsymbol{e}_z, \tag{22}$$

and the renormalized quantities in Eq. (21) are given by

$$\eta = \frac{m_ea^2}{\pi\hbar^2}\left(\frac{\Delta}{2} - 4\frac{m_e\lambda^2\epsilon_F}{\Delta}m_z^2\right),$$

where a is the lattice constant. The additional term in Eq. (22) is an anisotropic damping term which for the typical parameters (see Table II) we use in the calculation of the domain-wall dynamics is negligible; moreover these parameters also imply $\eta \ll 1$. Furthermore, we obtain that the observed Gilbert damping constant is given by

$$\alpha'_G = \alpha_G - \alpha\frac{a^2m_e}{\pi\hbar^2}\left[\epsilon_F - \frac{m_e\lambda^2}{2}\left(1-\frac{4\epsilon_F^2}{\Delta^2}\left(1+4m_z^2\right)\right)\right]. \tag{23}$$

Note that α_G phenomenologically describes the damping of the magnetzation due to interactions other than the s-d coupling, such as relaxation due to magnon-phonon interactions. Before we calculate the spin torques within this semiclassical framework we determine the current as a function of electric field within this simple model. We need this later on to express the spin torques in terms of the current.

IV. CONDUCTIVITY

In this section we give the conductivity for the Rashba system. Note that the conductivity we find here is correct only within this simple *s*-*d* description. We need the conductivity in order to interpret the current-induced torques in the next section. The conductivity σ_{ij} is defined as $j_c^i = \sigma^{ij} E^i$, where $\boldsymbol{j}_c$ is the charge-current density. We calculate the conductivity up to first order in the gradient of the magnetization and up to second order in the SO coupling strength. The expression for the charge-current density is given by

$$\boldsymbol{j}_c = -|e| \sum_{s=\pm} \int \frac{d^2\boldsymbol{p}}{(2\pi\hbar)^2} f_s(\boldsymbol{x},\boldsymbol{p},t)\dot{\boldsymbol{x}}_s. \tag{24}$$

Using the relaxation-time approximation described in the previous section, we find that the conductivity has three contributions, $\sigma = \sigma_0 + \sigma_{\mathrm{AH}} + \sigma_{\mathrm{AMR}}$, corresponding to the diagonal, anomalous Hall effect, and anisotropic magnetoresistance, respectively. The diagonal conductivity is given by

$$\frac{\sigma_0^{ij}}{G_0} = \left(\frac{\epsilon_F \tau_r}{\hbar} + \alpha \frac{4 m_e \lambda^2 \epsilon_F}{\Delta^2}\right) \delta^{ij}, \tag{25}$$

where $G_0 = 2|e|^2/h$ is the quantum of conductance. The second contribution

$$\frac{\sigma_{\mathrm{AH}}^{ij}}{G_0} = \left[\frac{2 m_e \lambda^2}{\Delta} m_z + \lambda \tau_r \left(\boldsymbol{m}\cdot(\boldsymbol{\nabla}\times\boldsymbol{m}) - \alpha \frac{2\epsilon_F}{\Delta}(\boldsymbol{\nabla}\cdot\boldsymbol{m})\right)\right]\epsilon^{ijz}, \tag{26}$$

which is the anomalous Hall response generalized to inhomogeneous magnetization. The last contribution to the conductivity is

$$\frac{\sigma_{\mathrm{AMR}}^{ij}}{G_0} = m_e \lambda^2 \left(\alpha \frac{4\epsilon_F}{\Delta^2} - \frac{\tau_r}{\hbar}\right) \epsilon^{iaz}\epsilon^{jbz} m^a m^b, \tag{27}$$

which depends on the relative orientation of the electric field and the magnetization and hence corresponds to anisotropic magnetoresistance. We also define the current polarization via

$$\mathcal{P}\boldsymbol{j}_c \equiv -|e| \sum_{s=\pm} \int \frac{d^2\boldsymbol{p}}{(2\pi\hbar)^2} f(\epsilon_s) s \dot{\boldsymbol{x}}_s,$$

for later reference.

V. CURRENT-INDUCED TORQUES

In this section we give the current-induced torques for the Rashba model, introduced in Sec. III. The current-induced torques can be calculated from the current-induced spin density. They are given by

$$\begin{aligned}\boldsymbol{\tau}_{\mathrm{ST}} &= \frac{\Delta}{2\hbar}\boldsymbol{m}\times\langle\boldsymbol{s}\rangle \\ &= \frac{\Delta a^2}{2\hbar}\boldsymbol{m}\times\sum_{s=\pm}\int\frac{d^2\boldsymbol{p}}{(2\pi\hbar)^2} f_s(\boldsymbol{x},\boldsymbol{p},t)\boldsymbol{s}_s,\end{aligned} \tag{28}$$

where $\boldsymbol{\tau}_{\mathrm{ST}}$ is the sum of all the separate spin torques we list below. We evaluate the integral in Eq. (28) up to first order in the damping parameter α and gradient of the magnetization and up to second order in the spin-orbit-coupling strength λ. Note that we include only terms linear in the electric field, and that we take $\partial\boldsymbol{m}/\partial t = 0$. Taking into account this time dependence gives rise to the renormalization of damping and gyromagnetic ratio that we already discussed in the previous section.

In agreement with our phenomenological arguments [see Eqs. (8) and (9)], we obtain two spin torques that are zeroth order in the gradient of the magnetization, which are given by

$$\boldsymbol{\tau}^{(1)} = \frac{|e| m_e \lambda a^2}{\pi\hbar^2}\left(\frac{\Delta\tau_r}{2\hbar} - \alpha\frac{2\epsilon_F}{\Delta}\right)(\boldsymbol{E}\times\boldsymbol{e}_z)\times\boldsymbol{m}; \tag{29}$$

$$\boldsymbol{\tau}^{(1\perp)} = \frac{|e| m_e \lambda a^2}{\pi\hbar^2}[(\boldsymbol{E}\times\boldsymbol{e}_z)\times\boldsymbol{m}]\times\boldsymbol{m}. \tag{30}$$

These homogeneous SO-induced spin torques were derived before.[12,18] In the case $\alpha = 0$, we agree with Manchon and Zhang[12] and with Kim *et al.*[18] about the ratio between the reactive and dissipative torques. In addition, for $\alpha \neq 0$, we find another contribution to these torques coming from spin relaxation. Note that the two torques given above form a perpendicular pair, one dissipative and one reactive. In what follows we will group the torques into these pairs when both reactive and dissipative torques emerge to second order in SO coupling.

All other torques are first order in the gradient of the magnetization. The first two torques we find are given by

$$\boldsymbol{\tau}^{\mathrm{STT}} = -\frac{|e|\tau_r a^2}{\pi\hbar^2}\left(\frac{\Delta}{2} + 2\frac{\alpha\hbar m_e\lambda^2}{\tau_r\Delta} - 12 m_e\lambda^2\frac{\epsilon_F}{\Delta}\right)\times(\boldsymbol{E}\cdot\boldsymbol{\nabla})\boldsymbol{m}; \tag{31}$$

$$\boldsymbol{\tau}^{\mathrm{STT}\perp} = \frac{|e|\alpha\tau_r a^2}{\pi\hbar^2}\left[\epsilon_F + \frac{m_e\lambda^2}{2}\left(7 + \frac{4\epsilon_F^2}{\Delta^2}\left(3 + 4m_z^2\right)\right)\right]\boldsymbol{m}\times(\boldsymbol{E}\cdot\boldsymbol{\nabla})\boldsymbol{m}, \tag{32}$$

which are the well-known STTs that also occur in systems with negligible SO coupling [see Eq. (4)] and are due to the spin-polarized current in the direction of the electric field. The ratio of these two torques defines the β parameter. We find that

$$\beta = -\frac{2\alpha}{\Delta}\left[\epsilon_F + m\lambda_R^2\left(\frac{7}{2} + \frac{\epsilon_F^2}{\Delta^2}(30 + 8m_z^2)\right)\right]. \tag{33}$$

In the previous section we showed that the current can be decomposed into three components. Several of the torques we find can be interpreted as the ordinary spin transfer torques [Eq. (4)] with current response modified due to the SO coupling. First, we have the torques

$$-\frac{4|e| m_e \epsilon_F \lambda^2 a^2}{\pi\Delta^2\hbar}(\boldsymbol{m}\cdot\boldsymbol{e}_z)[(\boldsymbol{E}\times\boldsymbol{e}_z)\cdot\boldsymbol{\nabla}]\boldsymbol{m};$$

$$\frac{2|e| m_e \alpha\lambda^2 a^2}{\pi\Delta\hbar}(\boldsymbol{m}\cdot\boldsymbol{e}_z)\boldsymbol{m}\times[(\boldsymbol{E}\times\boldsymbol{e}_z)\cdot\boldsymbol{\nabla}]\boldsymbol{m},$$

which are due to the anomalous Hall current $j_{\mathrm{AH}}^i \equiv \sigma_{\mathrm{AH}}^{ij} E^j$, and can therefore be written as

$$\boldsymbol{\tau}^{\mathrm{AH}} = \mathcal{P}(\boldsymbol{j}_{\mathrm{AH}}\cdot\boldsymbol{\nabla})\boldsymbol{m}; \tag{34}$$

$$\boldsymbol{\tau}^{\mathrm{AH}\perp} = \mathcal{P}\frac{\alpha\Delta}{2\epsilon_F}\boldsymbol{m}\times(\boldsymbol{j}_{\mathrm{AH}}\cdot\boldsymbol{\nabla})\boldsymbol{m}. \tag{35}$$

Two torques can be interpreted to be a generalization of the STTs coming from the anisotropic magnetoresistance response given by Eq. (27). These torques are

$$\boldsymbol{\tau}^{\mathrm{AMR}} = -\frac{2|e|m_e\lambda^2 a^2}{\pi\Delta\hbar}\left(\alpha - 24\frac{\epsilon_F\tau_r}{\hbar}\right)[(\boldsymbol{E}\times\boldsymbol{e}_z)\cdot\boldsymbol{m}] \times[(\boldsymbol{m}\times\boldsymbol{e}_z)\cdot\nabla]\boldsymbol{m}; \tag{36}$$

$$\boldsymbol{\tau}^{\mathrm{AMR}\perp} = -\frac{|e|m_e\lambda^2\alpha\tau_r a^2}{\pi\hbar^2}\left(5 + 16\frac{\epsilon_F^2}{\Delta^2}\right)[(\boldsymbol{E}\times\boldsymbol{e}_z)\cdot\boldsymbol{m}]\boldsymbol{m} \times[(\boldsymbol{m}\times\boldsymbol{e}_z)\cdot\nabla]\boldsymbol{m}. \tag{37}$$

The next torque, given by

$$\boldsymbol{\tau}^{\mathrm{Hall}} = -\frac{|e|m_e\lambda^2\alpha\tau_r a^2}{2\pi\hbar^2}\left(1 + 4\frac{\epsilon_F^2}{\Delta^2}\right)[(\boldsymbol{E}\times\boldsymbol{m})\cdot\nabla]\boldsymbol{m}, \tag{38}$$

has the symmetry of a STT due to a normal Hall response. This is not the normal Hall response because it is quadratic in the SO-coupling parameter. In our description we did not include the normal Hall response of the system, due to the smallness of the effect.

The torques obtained up to this point could be interpreted as the known SO-coupling-induced spin torques for Eqs. (29) and (30) and the STTs [in Eqs. (31)–(38)] with a current response that is modified due to SO coupling. Now we will list the torques that cannot be interpreted as known current-induced torques. We have the pairs

$$\boldsymbol{\tau}^{\mathrm{a}} = \frac{2|e|m_e\lambda^2 a^2}{\pi\Delta\hbar}\left(\frac{\epsilon_F\tau_r}{\hbar} - \alpha\right)[\boldsymbol{m}\times(\boldsymbol{E}\times\boldsymbol{e}_z)]^a\boldsymbol{m} \times(\boldsymbol{e}_z\times\nabla)m^a; \tag{39}$$

$$\boldsymbol{\tau}^{\mathrm{a}\perp} = -\frac{4|e|m_e\epsilon_F\lambda^2 a^2}{\pi\Delta^2\hbar}[\boldsymbol{m}\times(\boldsymbol{E}\times\boldsymbol{e}_z)]^a\boldsymbol{m} \times[\boldsymbol{m}\times(\boldsymbol{e}_z\times\nabla)]m^a, \quad \text{and} \tag{40}$$

$$\boldsymbol{\tau}^{\mathrm{b}} = -2\frac{\alpha|e|m_e\lambda^2 a^2}{\pi\hbar}\frac{\tau_r}{\hbar}(\boldsymbol{E}\times\boldsymbol{e}_z)^a\boldsymbol{m}\times(\boldsymbol{e}_z\times\nabla)m^a; \tag{41}$$

$$\boldsymbol{\tau}^{\mathrm{b}\perp} = \frac{2|e|m_e\lambda^2 a^2}{\pi\Delta\hbar}\left(\alpha - \frac{\epsilon_F\tau_r}{\hbar}\right)(\boldsymbol{E}\times\boldsymbol{e}_z)^a\boldsymbol{m} \times[\boldsymbol{m}\times(\boldsymbol{e}_z\times\nabla)]m^a. \tag{42}$$

We also have four torques that do not form reactive-dissipative pairs, listed below:

$$\boldsymbol{\tau}^{\mathrm{c}} = 4\frac{|e|m_e\epsilon_F\lambda^2\tau_r a^2}{\pi\Delta\hbar^2}(\boldsymbol{m}\cdot\nabla\boldsymbol{m}\cdot\boldsymbol{e}_z)\boldsymbol{m}\times(\boldsymbol{E}\times\boldsymbol{e}_z); \tag{43}$$

$$\boldsymbol{\tau}^{\mathrm{d}} = -4\frac{|e|m_e\epsilon_F\lambda^2\tau_r a^2}{\pi\Delta\hbar^2}(\boldsymbol{E}\times\boldsymbol{e}_z)^a(\boldsymbol{m}\cdot\nabla)m^a(\boldsymbol{m}\times\boldsymbol{e}_z); \tag{44}$$

$$\boldsymbol{\tau}^{\mathrm{e}} = \frac{|e|m_e\lambda^2\alpha\tau_r a^2}{\pi\hbar^2}\left(1 + 4\frac{\epsilon_F^2}{\Delta^2}\right)E^a(\boldsymbol{m}\times\nabla)m^a; \tag{45}$$

$$\boldsymbol{\tau}^{\mathrm{f}} = \frac{3|e|m_e\lambda^2\alpha\tau_r a^2}{2\pi\hbar^2}\left(1 + 4\frac{\epsilon_F^2}{\Delta^2}\right)\boldsymbol{e}_z^a(\boldsymbol{m}\times\boldsymbol{e}_z)(\boldsymbol{E}\cdot\nabla)m^a, \tag{46}$$

When we discussed all the possible torques in Sec. II B we always obtained pairs of a reactive and a dissipative torque.

TABLE I. Magnetic anisotropy configuration and the corresponding domain-wall structures.

	Easy axis (K)	Hard axis ($K_\perp$)
Bloch (z)	z	y
Néel (x)	x	z
Bloch (y)	y	x

There we looked only at the torques that respect the symmetries of the system. That not all the torques we obtained via the semiclassical approximation form reactive-dissipative pairs means that within this approximation some of the allowed torques are not realized. Note that the above torques are of second order in $\boldsymbol{e}_z$, and have therefore not been explicitly written down in Sec. II B. The current-induced spin torques in this section are the central result of this paper. From the list of torques we presented here it is clear that the interplay of SO coupling and an inhomogeneous magnetization gives rise to many spin torques. In the next section we consider their effect on current-induced domain-wall motion.

VI. DOMAIN-WALL MOTION

In this section we investigate the effect the spin torques have on current-induced domain-wall dynamics. We study the domain-wall dynamics by employing the one-dimensional rigid domain-wall model. Within this model the dynamics is captured by the collective coordinates of the wall which are its position r_{DW} and central angle φ_{DW}. We study three different realizations of domain walls summarized in Table I. Due to the SO coupling the current-driven motion of the three walls differs. In order to arrive at the equations of motion for the collective coordinates we describe the direction of the magnetization $\boldsymbol{m} = (\cos\varphi_{\mathrm{DW}}\sin\theta_{\mathrm{DW}}, \sin\varphi_{\mathrm{DW}}\sin\theta_{\mathrm{DW}}, \cos\theta_{\mathrm{DW}})$ using two angles θ_{DW} and φ_{DW}. We use $\theta_{\mathrm{DW}}(x,t) = 2\arctan\{\exp[x - r_{\mathrm{DW}}(t)]/\lambda_{\mathrm{DW}}\}$ and the time-dependent but spatially homogenous $\varphi_{\mathrm{DW}}(t)$, where $\lambda_{\mathrm{DW}} = \sqrt{J/K}$ is the domain-wall width in terms of the exchange stiffness J and the easy-axis anisotropy K. This description of the domain wall is rigid, that is, the domain wall can only move or rotate. The direction of the electric field is specified by the angle ϕ_E with the x axis in the x-y plane. The known[13,24] equations of motion for the collective coordinates r_{DW} and φ_{DW} are augmented by terms obtained from the current-induced torques of the previous section. In the calculations we make use of the parameter values as given in Table II. These parameters are typical for metallic ferromagnets, and the value of the spin-orbit coupling

TABLE II. Parameters used in domain-wall motion calculations.

ϵ_F	=	1 eV
Δ	=	0.1 eV
$m\lambda^2$	=	9 meV
α'_G	=	0.05
α	=	0.05
τ	=	30 fs
λ_{DW}	=	10 nm
a	=	0.3 nm

is taken from Ref. 16. Furthermore, we give the results as a function of the critical field E_c and velocity v_c for the case without SO coupling, which are defined as[24]

$$v_c = \frac{K_\perp}{\hbar}\lambda_{\rm DW}; \quad E_c = \frac{v_c}{\mu_s^0}, \tag{47}$$

where the spin mobility in the absence of SO coupling is defined as

$$\mu_s^0 = -\frac{|e|\tau_r \Delta a^2}{2\pi\hbar^2},$$

which is the zero-SO-coupling ($\lambda \to 0$) limit of Eq. (31). In Eq. (21) we introduced the renormalized Gilbert damping parameter α_G', which is the Gilbert damping parameter that will be measured in experiments. We expect that the Gilbert damping α_G for the magnetization and the damping α for the itinerant spins are of the same order of magnitude. In the Appendix we give the equations of motion for the Néel (x) and Bloch (y) wall configurations. Here we explicitly address the Bloch (z) wall.

The equations of motion for the collective coordinates are obtained by inserting the Bloch (z) domain-wall ansatz, as given above, into the equation of motion for the magnetization [see Eq. (21)]. To get the equations of motion we take the inner product with $\delta \boldsymbol{m}_{\rm Bloch(z)}/\delta r_{\rm DW}$, for one equation of motion and similarly for $\delta \boldsymbol{m}_{\rm Bloch(z)}/\delta\varphi_{\rm DW}$. Subsequently we integrate those two equations over all space. The two equations of motion we obtain in this way are given below:

$$\frac{\dot r_{\rm DW}}{\lambda_{\rm DW}} - \alpha_G'\dot\varphi_{\rm DW} - \frac{K_\perp}{\hbar}\sin 2\varphi_{\rm DW} = \left(\frac{\pi}{2}\tau^{(1)} + \frac{6\tau^{\rm a} + 4\tau^{\rm c}}{6\lambda_{\rm DW}}\cos\varphi_{\rm DW} - \frac{\tau^{\rm e}}{3\lambda_{\rm DW}}\sin\varphi_{\rm DW}\right) E\cos(\phi_E - \varphi_{\rm DW}) + \frac{2\tau^{\rm b\perp} - 4\tau^{\rm AMR}}{6\lambda_{\rm DW}} E\sin(\phi_E - \varphi_{\rm DW})\sin\varphi_{\rm DW} - \frac{\tau^{\rm STT}}{\lambda_{\rm DW}} E\cos\phi_E; \tag{48}$$

$$\dot\varphi_{\rm DW} + \alpha_G'\frac{\dot r_{\rm DW}}{\lambda_{\rm DW}} = \left(\frac{\pi}{2}\tau^{(1\perp)} - \frac{\tau^{\rm a\perp}}{\lambda_{\rm DW}}\cos\varphi_{\rm DW}\right) E\cos(\phi_E - \varphi_{\rm DW}) + \frac{4\tau^{\rm AMR\perp} + 2\tau^{\rm b}}{3\lambda_{\rm DW}} E\sin(\phi_E - \varphi_{\rm DW})\sin\varphi_{\rm DW} + \frac{2\tau^{\rm f} + 3\tau^{\rm STT\perp}}{3\lambda_{\rm DW}} E\cos\phi_E. \tag{49}$$

The scalars $\tau^{(i)}$ are defined as the prefactors in front of the vector quantities of the torques in Sec. V.

The boundary conditions for the current through the ferromagnet are such that only a current in the x direction is present. In the figures we took $\phi_E = 0$, since the off-diagonal contributions in the conductivity give rise to a small (<1% of the external field for the parameters used) voltage gradient in the y direction. The average domain-wall velocity is defined as $v_{\rm DW} = \langle \dot r_{\rm DW}\rangle$, where the angular brackets denote a long-time average.

A. Interpretation of domain-wall motion

The results in Figs. 1–3 show that the inclusion of spin torques due to the combined effect of SO coupling and an inhomogenous magnetization changes the domain-wall mobility $\mu_{\rm DW} = dv_{\rm DW}/dE$ completely as compared to the situation without these torques.

In Fig. 1 we show the average Bloch (z)–wall velocity as a function of the applied electric field in the x direction. The different lines correspond to the following situations: The blue dashed and dot-dashed lines correspond to current-driven domain-wall motion without torques induced by SO coupling, i.e., only the STTs. The dashed line is the result of the limit $\lambda_R \to 0$ of Eqs. (48) and (49).

In Sec. III we obtained a renormalized version of the LLG equation [see Eq. (21)] due to SO coupling, and in Sec. V we showed that the parameter β also depends on the strength of the SO coupling as can be seen from Eq. (33). The dot-dashed line shows the result for keeping only the STTs in the equation of motion but with the parameters renormalized by the SO coupling. The dotted black line is the result with the STTs and the homogeneous SO-coupling-induced torques in Eqs. (29) and (30). The solid red line is the result for the full equations of motion in Eqs. (48) and (49).

In Fig. 1 we see that the SO coupling splits the Walker breakdown in two. Before Walker breakdown the domain-wall angle is time independent, $\varphi_{\rm DW}(t) = \phi_{\rm DW}$, where $\phi_{\rm DW}$ is the local minimum of a tilted washboard potential as shown in the inset. This tilted washboard potential $V(\varphi_{\rm DW})$ is obtained by eliminating $\dot r_{\rm DW}$ from Eqs. (48) and (49), such that we obtain the equation of motion $\dot\varphi_{\rm DW} = -dV(\varphi_{\rm DW})/d\varphi_{\rm DW}$. When the domain-wall angle is in a local minimum of the washboard potential, $\dot\varphi_{\rm DW} = 0$. Without SO coupling the washboard is formed by the anisotropy energy only and the tilting is due to the applied field E. When we add SO coupling to the equation, the field also changes the washboard potential, leading to inequivalent local minima. This explains the splitting of the Walker breakdown for the Bloch (z) domain wall structure.

After Walker breakdown the asymptotic domain-wall velocities are determined by the effective mobility, which is simply μ_s^0 in the case without SO coupling. The effective mobility for the case with only the homogeneous SO-induced torques is the same as the mobility for renormalized current-induced domain-wall motion with STTs only, which can be seen by the asymptotic behaviour of the dot-dashed and dotted lines. When we include all torques induced by the SO coupling not only the magnitude but also the sign of this effective

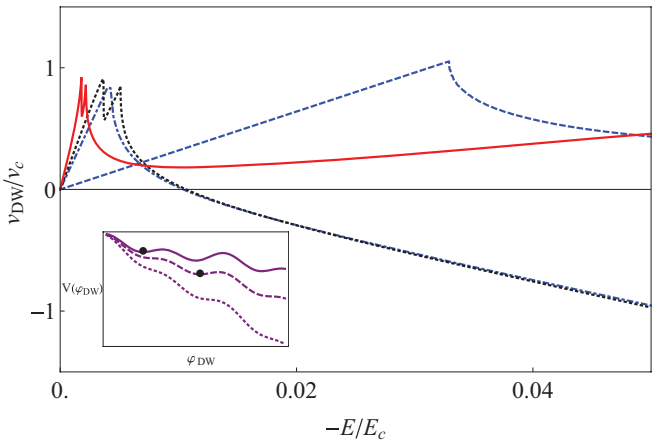

FIG. 1. (Color online) Average velocity of a Bloch (z) wall as a function of the applied field. The dashed (blue) line is the situation without SO coupling ($\lambda_R = 0$), the dot-dashed (blue) line represents current-driven domain-wall motion without torques induced by the SO coupling but with the parameters renormalized by the SO coupling, and the dotted (black) line shows the results with only the homogeneous SO torques, i.e., $\boldsymbol{\tau}^{(1)}$ and $\boldsymbol{\tau}^{(1\perp)}$ added to the STTs. The solid (red) line shows the result of the solution of the equations of motion including all spin torques. The parameters used to obtain these results are given in Table II. The inset is an illustration of the tilted washboard potential of the φ_{DW} coordinate for increasing values of applied field. Due to the SO coupling there are inequivalent local minima. The angle points in the direction of the first local minimum, with slightly more field the angle makes a fast rotation to the second minimum. Above Walker breakdown there are no more local minima and the angle rotates in time.

mobility changes with respect to the previously discussed cases. The effective mobility is hard to calculate since the tilted washboard potential for the domain-wall angle is nonlinearly dependent on the applied field.

In Figs. 2 and 3 we show the results for the Néel (x) and Bloch (y) walls, respectively. It is clear that also in these cases the additional torques induce qualitatively different behaviour of the domain-wall motion compared to the situation with only the torques induced by SO coupling for homogeneous magnetization.

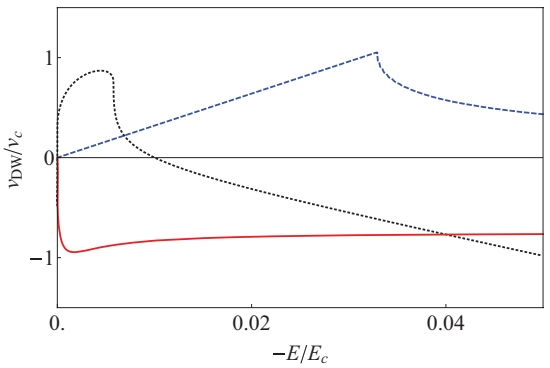

FIG. 2. (Color online) Average velocity of a Néel (x) wall as a function of applied electric field in the x direction. Lines are as in Fig. 1. The equations of motion can be found in the Appendix.

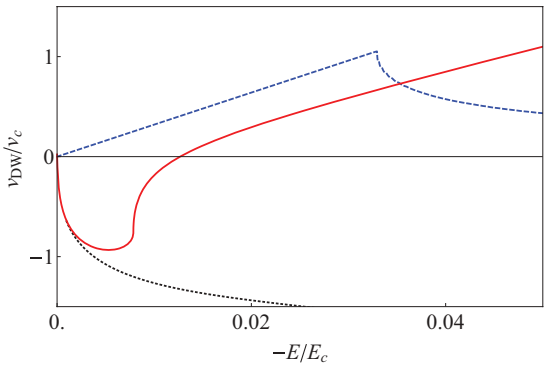

FIG. 3. (Color online) Average velocity of a Bloch (y) wall as a function of applied electric field in the x direction. Lines are as in Fig. 1. The equations of motion can be found in the Appendix.

VII. DISCUSSION

In this paper we considered Rashba SO coupling. Our results can be generalized straightforwardly to linear Dresselhaus SO coupling,[25] which is linear in momentum too. For linear Dresselhaus coupling the dispersion of the carriers is the same as for Rashba coupling. The effective magnetization for the Dresselhaus SO coupling is given by $\boldsymbol{\Omega}_D(\boldsymbol{x},\boldsymbol{p}) = \Delta\boldsymbol{m}/2 + \lambda_D(-p_x,p_y,0)^T$. This means $\boldsymbol{p}\times\boldsymbol{e}_z \rightarrow (-p_x,p_y,0)^T$ when we go from the Rashba to the Dresselhaus coupling. The current-induced torques we found in Sec. V involve factors $\boldsymbol{v}\times\boldsymbol{e}_z$, where $\boldsymbol{v}$ is a vector. For clarity we consider $\boldsymbol{\tau}^{(1)} \propto (\boldsymbol{E}\times\boldsymbol{e}_z)\times\boldsymbol{m}$ [given in Eq. (29)]; for the Dresselhaus system the torque would be in the direction $(\boldsymbol{E}\times\boldsymbol{e}_z)\times\boldsymbol{m} \rightarrow (-E_x,E_y,0)\times\boldsymbol{m}$. In this way we obtain the results for the textured Dresselhaus ferromagnet. The results for combined Rashba-Dresselhaus SO coupling are less straightforward to obtain since the dispersion of the carriers changes.

Another obvious place to look for the appearance of additional torques due to SO coupling would be in dilute magnetic semiconductor systems, where the effective Hamiltonian for the carriers also has strong SO coupling. In Ref. 26 spin torques for the dilute limit are calculated for this system. In that work one of the current-induced torques is interpreted as an anisotropic dissipative STT. This anisotropic torque can as well be interpreted as the torque given by Eq. (15). It would be very interesting to see which other torques would appear in those systems.

The reciprocal physical mechanism associated with current-induced torques are currents driven by nonequilibrium magnetization dynamics, often referred to as spin-motive forces. We obtain these using the Onsager reciprocal relations.[27] We do this via the linear-response matrix

$$\begin{pmatrix} \dot{m}^i \\ j_c^i \end{pmatrix} = \begin{pmatrix} m^k\epsilon^{ijk} & L^{ij}_{\mathrm{CIT}}(\boldsymbol{m},\boldsymbol{e}_z,\nabla\boldsymbol{m}) \\ L^{ij}_{\mathrm{SMF}}(\boldsymbol{m},\boldsymbol{e}_z\nabla\boldsymbol{m}) & \sigma^{ij}(\boldsymbol{m},\boldsymbol{e}_z,\nabla\boldsymbol{m}) \end{pmatrix} \cdot \begin{pmatrix} H^j_{\mathrm{eff}} \\ E^j \end{pmatrix},$$

where $L^{ij}_{\mathrm{CIT}}(\boldsymbol{m},\boldsymbol{e}_z,\nabla\boldsymbol{m})$ is the (3×3) matrix that gives the current-induced torques as defined in Eq. (7) and $L^{ij}_{\mathrm{smf}}(\boldsymbol{m},\boldsymbol{e}_z,\nabla\boldsymbol{m})$ gives the spin-motive forces. These two

matrices are related via Onsager reciprocity, which yields

$$L^{ij}_{\mathrm{CIT}}(\boldsymbol{m},\boldsymbol{e}_z,\nabla\boldsymbol{m}) = L^{ji}_{\mathrm{SMF}}(-\boldsymbol{m},\boldsymbol{e}_z,-\nabla\boldsymbol{m}).$$

VIII. CONCLUSION

We considered current-induced torques in systems that have SO coupling and a textured magnetization. The effects of these torques on domain-wall motion have been investigated. We have shown that the effects of the interplay between the SO coupling and the gradients in the magnetization are qualitatively important for domain-wall dynamics. In particular, we showed that the inclusions of all torques typically changes the domain-wall mobility as compared to including only the spin transfer torques that occur at weak spin-orbit coupling and/or the homogeneous spin torques due to SO coupling. The results of this work may be used to discriminate between Rashba SO coupling and injection of a spin current via the spin-Hall effect, because the latter will show only the homogeneous current-induced torques.

In future work we intend to explore in more detail the spin-motive forces that arise due to SO coupling. Another interesting direction for future research is the inclusion of thermal gradients and heat currents.

ACKNOWLEDGMENTS

It is a pleasure to thank Arne Brataas and Dima Pesin for useful remarks. This work was supported by the Stichting voor Fundamenteel Onderzoek der Materie (FOM), the Netherlands Organization for Scientifc Research (NWO), and the European Research Council (ERC).

APPENDIX: DIFFERENT DOMAIN-WALL CONFIGURATIONS

In this Appendix we give the equations of motion for the Néel (x) and Bloch (y) domain-wall configurations. The magnetic anisotropy configurations corresponding to these different walls are given in Table I.

1. Néel (x) wall

The Néel (x) wall is parametrized as $\boldsymbol{m} = (\cos[\theta(\boldsymbol{x},t)], \cos\phi(\boldsymbol{x},t)\sin[\theta(\boldsymbol{x},t)], \sin\phi(\boldsymbol{x},t)\sin[\theta(\boldsymbol{x},t)])^T$. The equations of motion are obtained as explained in Sec. VI of the main text. The equations of motion for the collective coordinates are given by

$$\frac{\dot{r}_{\mathrm{DW}}}{\lambda_{\mathrm{DW}}} - \alpha'_G\dot{\varphi}_{\mathrm{DW}} = \frac{K_\perp}{\hbar}\sin 2\varphi_{\mathrm{DW}} - \left(\tau^{(1\perp)} + \frac{1}{3\lambda_{\mathrm{DW}}}\tau^{\mathrm{e}}\cos^2\varphi_{\mathrm{DW}} + \frac{\pi}{4\lambda_{\mathrm{DW}}}\left(\tau^{\mathrm{AH}} - \tau^{\mathrm{b}} + \tau^{\mathrm{Hall}}\right)\sin\varphi_{\mathrm{DW}}\right)E\sin\phi_E$$
$$- \left(\frac{\pi}{2}\tau^{(1)}\sin\varphi_{\mathrm{DW}} + \frac{1}{3\lambda_{\mathrm{DW}}}\left(\tau^{\mathrm{b}\perp} + \tau^{\mathrm{d}} - 2\tau^{\mathrm{AMR}}\right)\cos^2\varphi_{\mathrm{DW}} - \frac{1}{3\lambda_{\mathrm{DW}}}(3\tau^{\mathrm{a}} + \tau^{\mathrm{c}})\sin^2\varphi_{\mathrm{DW}} + \frac{\tau^{\mathrm{STT}}}{\lambda_{\mathrm{DW}}}\right)E\cos\phi_E,$$

$$\dot{\varphi}_{\mathrm{DW}} + \alpha'_G\frac{\dot{r}_{\mathrm{dw}}}{\lambda_{\mathrm{DW}}} = \frac{1}{\lambda_{\mathrm{DW}}}\left[\frac{\pi}{2}\left(\frac{1}{2}\tau^{\mathrm{e}} - \lambda_{\mathrm{DW}}\tau^{(1\perp)}\right)\sin\varphi_{\mathrm{DW}} - \frac{1}{3}\left[\left(2\tau^{\mathrm{AMR}} + \tau^{\mathrm{b}}\right)\cos^2\varphi_{\mathrm{DW}} - \left(-3\tau^{\mathrm{a}\perp} + \tau^{\mathrm{f}}\right)\sin^2\varphi_{\mathrm{DW}}\right] + \tau^{\mathrm{STT}\perp}\right]E\cos\phi_E$$
$$+ \left(\tau^{(1)} + \frac{\pi}{16\lambda_{\mathrm{DW}}}(4\tau^{\mathrm{AH}\perp} - 4\tau^{\mathrm{b}\perp} - \tau^{\mathrm{c}} - \tau^{\mathrm{d}})\sin\varphi_{\mathrm{DW}}\right)E\sin\phi_E.$$

2. Bloch (y) wall

For the Bloch wall the magnetization is parametrized as $\boldsymbol{m} = (\cos\phi(\boldsymbol{x},t)\sin[\theta(\boldsymbol{x},t)], \cos[\theta(\boldsymbol{x},t)], \sin\phi(\boldsymbol{x},t)\sin[\theta(\boldsymbol{x},t)])^T$. The equations of motion are

$$\frac{\dot{r}_{\mathrm{DW}}}{\lambda_{\mathrm{DW}}} - \alpha'_G\dot{\varphi}_{\mathrm{DW}} - \frac{K_\perp}{\hbar}\sin 2\varphi_{\mathrm{DW}} = \frac{1}{3\lambda_{\mathrm{DW}}}(\tau^{\mathrm{AMR}} - 2\tau^{\mathrm{b}} - 3\tau^{\mathrm{STT}} - \tau^{\mathrm{d}}\sin^2\varphi_{\mathrm{DW}} + 3\lambda_{\mathrm{DW}}\tau^{(1)\perp})E\cos\phi_E$$
$$- \left(\frac{2}{3\lambda_{\mathrm{DW}}}\tau^{\mathrm{e}} + \frac{\pi}{4}(\tau^{\mathrm{AH}} - \tau^{\mathrm{a}\perp} + \tau^{\mathrm{Hall}} + 2\lambda_{\mathrm{DW}}\tau^{(1)})\cos\varphi_{\mathrm{DW}}\right)E\sin\phi_E,$$

$$\dot{\varphi}_{\mathrm{DW}} + \alpha'_G\frac{\dot{r}_{\mathrm{DW}}}{\lambda_{\mathrm{DW}}} = -\frac{1}{3\lambda_{\mathrm{DW}}}(\tau^{\mathrm{AMR}\perp} + 2\tau^{\mathrm{b}} + 3\lambda_{\mathrm{DW}}\tau^{(1)} - 3\tau^{\mathrm{STT}\perp} - \tau^{\mathrm{f}}\cos^2\varphi_{\mathrm{DW}})E\cos\phi_E$$
$$+ \frac{\pi}{32\lambda_{\mathrm{DW}}}(8\tau^{\mathrm{a}} + 8\tau^{\mathrm{AH}\perp} + \tau^{\mathrm{c}} + \tau^{\mathrm{d}} - 16\lambda_{\mathrm{DW}}\tau^{(1\perp)} - (\tau^{\mathrm{c}} + \tau^{\mathrm{d}})\cos 2\varphi_{\mathrm{DW}})\cos\varphi_{\mathrm{DW}}E\sin\phi_E.$$

*e.vanderbijl@uu.nl

[1] S. S. P. Parkin, M. Hayashi, and L. Thomas, Science **320**, 190 (2008).

[2] J. C. Slonczewski, J. Magn. Magn. Mater. **159**, L1 (1996).

[3] L. Berger, Phys. Rev. B **54**, 9353 (1996).

[4] S. Zhang and Z. Li, Phys. Rev. Lett. **93**, 127204 (2004).

[5] S. E. Barnes and S. Maekawa, Phys. Rev. Lett. **95**, 107204 (2005).

[6] Y. Tserkovnyak, H. J. Skadsem, A. Brataas, and G. E. W. Bauer, Phys. Rev. B **74**, 144405 (2006).

[7] H. Kohno, G. Tatara, and J. Shibata, J. Phys. Soc. Jpn. **75**, 113706 (2006).

[8] F. Piéchon and A. Thiaville, Phys. Rev. B **75**, 174414 (2007).

[9] R. A. Duine, A. S. Núñez, J. Sinova, and A. H. MacDonald, Phys. Rev. B **75**, 214420 (2007); R. A. Duine, *ibid.* **79**, 014407 (2009).

[10] L. Thomas, M. Hayashi, X. Jiang, R. Moriya, C. Rettner, and S. Parkin, Nature (London) **443**, 197 (2006); L. Heyne, M. Kläui, D. Backes, T. A. Moore, S. Krzyk, U. Rüdiger, L. J. Heyderman, A. Fraile Rodríguez, F. Nolting, T. O. Mentes, M. A. Niño, A. Locatelli, K. Kirsch, and R. Mattheis, Phys. Rev. Lett. **100**, 066603 (2008); M. Bolte, G. Meier, B. Krüger, A. Drews, R. Eiselt, L. Bocklage, S. Bohlens, T. Tyliszczak, A. Vansteenkiste, B. Van Waeyenberge, K. W. Chou, A. Puzic, and H. Stoll, *ibid.* **100**, 176601 (2008); L. Heyne, J. Rhensius, D. Ilgaz, A. Bisig, U. Rüdiger, M. Kläui, L. Joly, F. Nolting, L. J. Heyderman, J. U. Thiele, and F. Kronast, *ibid.* **105**, 187203 (2010).

[11] M. E. Lucassen, C. H. Wong, R. A. Duine, and Y. Tserkovnyak, Appl. Phys. Lett. **99**, 262506 (2011).

[12] A. Manchon and S. Zhang, Phys. Rev. B **78**, 212405 (2008); **79**, 094422 (2009).

[13] K. Obata and G. Tatara, Phys. Rev. B **77**, 214429 (2008).

[14] I. Garate and A. H. MacDonald, Phys. Rev. B **80**, 134403 (2009).

[15] K. M. D. Hals, A. K. Nguyen, and A. Brataas, Phys. Rev. Lett. **102**, 256601 (2009).

[16] I. Miron, K. Garello, G. Gaudin, P.-J. Zermatten, M. Costache, S. Auffret, S. Bandiera, B. Rodmacq, A. Schuhl, and P. Gambardella, Nature (London) **476**, 189 (2011); I. Miron, T. Moore, H. Szambolics, L. Buda-Prejbeanu, S. Auffret, B. Rodmacq, S. Pizzini, J. Vogel, M. Bonfim, A. Schuhl, and G. Gaudin, Nat. Mater. **10**, 419 (2011).

[17] L. Liu, O. J. Lee, T. J. Gudmundsen, D. C. Ralph, and R. A. Buhrman, arXiv:1110.6846.

[18] K.-W. Kim, S.-M. Seo, J. Ryu, K.-J. Lee, and H.-W. Lee, Phys. Rev. B **85**, 180404(R) (2012).

[19] D. A. Pesin and A. H. MacDonald, Phys. Rev. B **86**, 014416 (2012).

[20] J. Ryu, S.-M. Seo, K.-J. Lee, and H.-W. Lee, J. Magn. Magn. Mater. **324**, 1449 (2012).

[21] K. M. D. Hals and A. Brataas (private communication).

[22] E. I. Rashba, Fiz. Tverd. Tela (Leningrad) **2**, 1224 (1960).

[23] N. A. Sinitsyn, J. Phys.: Condens. Matter **20**, 023201 (2008); T. Jungwirth, Q. Niu, and A. H. MacDonald, Phys. Rev. Lett. **88**, 207208 (2002); E. van der Bijl and R. A. Duine, *ibid.* **107**, 195302 (2011).

[24] G. Tatara and H. Kohno, Phys. Rev. Lett. **92**, 086601 (2004); **96**, 189702 (2006).

[25] G. Dresselhaus, Phys. Rev. **100**, 580 (1955).

[26] D. Culcer, M. E. Lucassen, R. A. Duine, and R. Winkler, Phys. Rev. B **79**, 155208 (2009).

[27] C. H. Wong and Y. Tserkovnyak, Phys. Rev. B **80**, 184411 (2009).